Goldilocks and the three glymes: how Na⁺ solvation controls Na-O₂ battery cycling

N. Ortiz Vitoriano ^{1,2}*, I. Ruiz de Larramendi ³, R.L. Sacci ⁴, I. Lozano ^{1,3}, C.A. Bridges ⁴, O. Arcelus ¹, M. Enterría ¹, J. Carrasco ¹, T. Rojo ^{1,3}, G.M. Veith ⁴*

¹Center for Cooperative Research on Alternative Energies (CIC energiGUNE), Basque Research and Technology Alliance (BRTA), Parque Tecnológico de Alava, Albert Einstein 48, 01510 Vitoria-Gasteiz, Spain.

²Ikerbasque, Basque Foundation for Science, María Díaz de Haro 3, 48013 Bilbao, Spain.
 ³Departamento de Química Inorgánica, Facultad de Ciencia y Tecnología, Universidad del País Vasco (UPV/EHU) Barrio Sarriena s/n, 48940 Leioa - Bizkaia, Spain
 ⁴Chemical Sciences Division, Oak Ridge National Laboratory, Oak Ridge, TN, 37831, USA

e-mail: nortiz@cicenergigune.com, veithgm@ornl.com

ABSTRACT

In this work we report a framework to understand the role of solvent-salt interactions and how they mediate the performance of sodium-air/O₂ batteries. The utilization of suitable electrolyte materials remains a point of major concern within the research community, as their stability and decomposition pathways during cycling are intimately connected with capacity and cycle life. Glyme based solvents have been widely utilized in Na-O2 batteries, however, to date no clear correlation between solvent/electrolyte properties and battery performance has been given. Herein, we have examined the effect of glyme chain length (ethylene glycol dimethyl ether DME; diethylene glycol dimethyl ether, DEGDME; and tetraethylene glycol dimethyl ether, TEGME) on the cycling behaviour of Na-O₂ batteries and conclude that overall cell performance is highly dependent on solvent selection, salt concentration and rate of discharge/charge. We demonstrate how solvent selection helps define cell chemistry and performance by linking salt-solvent interactions to enthalpy of dissolution - and subsequently to sodium battery electrolyte properties - through the combination of both experimental and theoretical methodologies. The approaches detailed in this study could be used to predictively prepare electrolytes for Li-air batteries, other glyme-based electrochemical systems and low temperature applications.

KEYWORDS

Glyme-based electrolyte, solvation, coordination, cycle life, sodium-air batteries, low temperature electrolytes, metal-air electrolyte

INTRODUCTION

Research into new energy storage technologies, for both portable and stationary applications, has become an urgent necessity. Among all energy storage systems,[1] those utilizing electrochemical technologies have the most potential to impact global energy generation, storage and use.[2] First identified in 1991, Li-ion batteries (LiBs) made such a change possible by revolutionising portable electronic devices due to their high volumetric and gravimetric energy density.[3] The continuing growth of the Li-ion battery market,[4] however, is expected to create a bottleneck in the supply of lithium in the future. Consequently, there has been growing interest in research focused on developing "beyond lithium" battery technologies to augment, or in certain situations replace, LiBs.

In this scenario, Na-air/O₂ batteries (NABs) have the potential to make a step change thanks to their high specific energy density and high energy efficiency.[5] NABs rely on the electrochemical reduction/oxidation of molecular oxygen at the cathode surface. The inherent advantage of metal-air batteries is that the active material in the cathode is absorbed from the surrounding environment (O₂), giving metal-air batteries some of the highest theoretical energy densities of all battery systems. Typically, the configuration of the battery consists of a sodium-containing anode, a sodium-conducting organic electrolyte, and an air cathode. The main component studied in these batteries has been the air cathode (where research has focused on carbon), catalysts, and - to a lesser extent - redox mediators.[6–8] Sodium metal is commonly used as the negative electrode, although sodiated carbon has also been explored.[9] Considerable work has been carried out in order to elucidate the reaction mechanism in NABs,[10–12]which involves oxygen gas (O₂) dissolving into the electrolyte and forming O₂-, and then combines with Na⁺ to form sodium superoxide (NaO₂) (Na⁺ + O₂ + 1e⁻ \leftrightarrow NaO₂).[13] Other discharge products, such as sodium peroxide (Na₂O₂) and peroxide hydrate (Na₂O₂·H₂O), have also been reported in the literature.[14] The role of electrolytes, however,

has been barely investigated, with only a few studies into different sodium salt anions[15,16], concentrated electrolytes[17], ionic liquids[18–21], discharge product composition[22] and side reactions.[23–25] These studies demonstrate that the choice of the electrolyte greatly influences the discharge product chemistry and morphology, the deposition mechanism, the solvation effect of the ion pairs, the appearance of parasitic reactions due to electrolyte decomposition and the overall cell performance.[16]

It is, therefore, clear that the choice of the electrolyte, both salt and solvent, are crucial for the successful development of Na-O₂ batteries. Currently, the most widely used solvents in Na-O₂ studies are the glyme family because of their quasi-stability to superoxide attack[23] and relatively stability towards Na metal anode; glymes, however, can be prone to attack by oxygen moieties during the oxygen reduction reaction (ORR).[26] In most Na-O₂ studies the choice of glyme-based solvents seems arbitrary and often is left unexplained. Lutz et al.[27] elucidated the ORR mechanism varying the glyme chain length where the importance of a low desolvation barrier (TEGDME>DEGDME>DME) for successful growth of NaO₂ was highlighted; however, the charge process (oxygen evolution reaction (OER)) was left unexplored which is key to understand and develop high performing Na-O₂ batteries.

In this study we demonstrate that the selection of solvent and the salt concentration has a profound effect on the cell performance. The coordination number of different glymes measured by infrared spectroscopy and coupled with density functional theory (DFT) calculations revealed different solvation behavior. Moreover, the enthalpy of dissolution measured using isothermal microcalorimetry varies significantly as a function of solvent selection. In addition, the rechargeable nature of Na-O₂ batteries is governed by the formation and oxidation of NaO₂, making it vital to study the effect of the electrolyte in the presence of NaO₂, and also to prevent the formation of irreversible side products.

EXPERIMENTAL SECTION

Materials.

Sodium perchlorate (NaClO₄, 98%, Sigma Aldrich) was purchased from Aldrich and was dried under vacuum at 80 °C for 24h. Ethylene glycol dimethyl ether ($C_4H_{10}O_2$, DME; anhydrous, 99.5% Sigma-Aldrich), diethylene glycol dimethyl ether ($C_6H_{14}O_3$, DEGDME; (anhydrous, 99.5% Sigma-Aldrich) and tetraethylene glycol dimethyl ether ($C_{10}H_{22}O_5$, TEGDME; \geq 99.7% Sigma Aldrich) were dried over molecular sieves (3 Å) for 1 week. After drying the materials, both the salt and the solvents were transferred to an Ar-filled glove box ($H_2O < 0.1$ ppm, $O_2 < 0.1$ ppm, Jacomex, France) without exposure to air. The electrolyte solutions were prepared by mixing the NaClO₄ salt with the corresponding solvent (DME, DEGDME or TEGDME). The final water content of the electrolytes was determined by C20 Karl Fisher coulometer (Mettler Toledo) and was below 20 ppm.

Gas diffusion layer GDL H2315 was purchased from Quintech (Freudenberg) and was dried under vacuum at 100 °C overnight. Afterwards, it was stored in the Ar-filled glove box without exposure to air.

Measurements.

Fourier Transform Infrared (FTIR) experiments of the electrolyte solutions were conducted using a diamond attenuated total reflection (ATR) attachment on a Bruker ALPHA that resided in an Ar-filled glovebox (~21 °C). The electrolytes were prepared in the glove box and placed in on the diamond ATR window and covered with a lid to prevent evaporation. Each spectrum was recorded as an average of 254 scans and the change in refractive index due to salt addition was not corrected.

DFT calculations were done using the Becke's three parameters (B3)[28] exchange functional along with the Lee-Yang-Parr (LYP)[29] nonlocal correlation functional (B3LYP), implemented in the all electron code FHI-aims with numeric atom-centered orbital basis

sets.[30,31] The structures were generated using the builder tools of the molecular editor Virtual NanoLab. Different solvation configurations were considered by optimizing [Na— $(M)_n$ complexes (where n = 1, 2, 3, 4 for M = DME; n = 1, 2, 3 for M = DEGDME; and n = 1, 2, 3, 4 for M = DME; M = 1, 2, 3, 4 for M = 1, 21, 2 for M = TEGDME) using a trust radius enhanced version of the Broyden-Fletcher-Goldfarb-Shanno optimization algorithm, where the forces were minimized until a 10⁻⁴ eV/Å threshold was achieved. The vibration modes and simulated IR spectra were calculated by finite differences with displacement values of 0.0025 Å. We placed a 20 cm⁻¹ full width half maximum to simulate standard line broadening to the individual IR bands to better compare with experimental data. Given the fairly big size of some of the complexes (up to 75 atoms in total), we used "light" settings and "tier2" standard basis set in the FHI-aims[30,31] code for Na, C, O, and H. Generally, "tight" settings should be used for calculating vibrational frequencies, particularly for O and H containing systems, as numerical noise might impact the calculated vibrational modes, especially at high frequencies. Therefore, we assessed the accuracy of our considered integration grids by calculating the vibrational modes of DME with both "light" and "tight" settings (see Table SI1). The maximum difference between both integration grids is only 4.5 cm⁻¹. Moreover, below 1200 cm⁻¹ differences are, in general, smaller than 1 cm⁻¹. We can therefore safely assume that the use of "light" settings is accurate enough to compute vibrational frequencies on these systems.

A MS-80 Calvet isothermal calorimeter (Setaram Instrumentation) operated at 25 °C was used to measure the enthalpies of dissolution of NaClO₄ in DME, DEGDME, and TEGDME. Powders of approximately 45-70 mg of dried NaClO₄, weighed on a Mettler UMT2 balance with a linearity of 1 µg, were dissolved using 18 mL of solvent in the calorimeter (molality of ≈0.021-0.035 mol/kg; molarity of ≈0.021-0.032 mol/L). A reference holder was constructed containing solvent but no salt. Samples were loaded in an Ar-filled glove box in steel holders with Chemraz O-rings, removed, and exposed for less than 5 seconds to ingress of air before

attaching the extension shaft to the top of the holder, followed by immediate loading into the calorimeter. The sample and reference holders were allowed to equilibrate for several hours beyond the point at which the baseline became flat. Due to the strong reactivity of DME with O-rings, a second holder obtained from Setaram Instrumentation was used for this solvent. For the DME data collection, NaClO₄ was loaded in the glove box under a PTFE membrane for the sample holder, while the reference holder did not contain any salt. DME (15 mL) was loaded above the membrane for both sample and reference holders and sealed; to measure the dissolution, the membranes were broken with a rod, followed by mechanical stirring to rapidly dissolve the salt in the sample holder. KCl was used to calibrate the calorimeter through dissolution in water at 25 °C; this was performed for both steel and Hastelloy holders. The Calisto software (Setaram Instrumentation) was used to determine the total heat flow by integrating the deviation from a linear baseline fit.

A pressurized 2-electrode Swagelok-type cell was used for the galvanostatic measurements. The cells were dried overnight at 120 °C and transferred to the glovebox prior to assembly. The Na-O₂ cells consisted of a sodium metal anode (12 mm ϕ , 99.9% Aldrich), GDL air cathode (12 mm ϕ , Quintech) and Celgard H2010 separators (Celgard, USA, 13 mm ϕ) soaked in 150 μ l of electrolyte (either 0.1 or 1.5 M NaClO₄ in DME, DEGDME and TEGDME solvents). A 12mm in diameter stainless steel mesh (Alfa Aesar) was used as the current collector. Following assembly, the cells were purged with pure oxygen to ~1 atm before the electrochemical measurements. Afterwards, cells were rested at open circuit voltage (~2.2 – 2.3 V vs Na⁺/Na) for 8 h prior to applying current in a Biologic-SAS VSP potentiostat. The discharge and charge experiments were performed at a current of 65 and 120 μ A to 0.5 mAh cm⁻² with a potential cut-off between 1.8 to 3.2 V vs Na⁺/Na.

Immediately after discharge, the electrodes were extracted from the cell and washed with dry DME. X-ray diffraction measurements on discharged electrodes were collected using a Bruker

D8 Discover diffractometer with $\theta/2\theta$ Bragg-Brentano geometry (monochromatic Cu radiation: $K_{\alpha 1} = 1.54056$ Å) within the 2θ range of 30 - 60° with an air tight sample holder (in-house made). Morphological characterization of the discharged and cycled electrodes was conducted by Scanning Electron Microscopy (SEM) using a FEI Quanta250 microscope operating at 20 kV. The electrodes were transferred from an Ar-filled glove box to the SEM using an air-tight holder to avoid air exposure.

RESULTS AND DISCUSSION

Coordination structure of NaClO₄ in DME/DEGDME/TEGDME: Theoretical and experimental approach.

When dissolving the sodium salt (NaClO₄) in the corresponding solvent (DME, DEGDME, TEGDME), a series of different interactions arise: i) cation-solvent; ii) anion-solvent and iii) cation-anion. Prior to the formation of these new ion-solvent dipole interactions, it is necessary to break the cation-anion electrostatic interaction; after which, the solvent and anion will compete to bind to the cation. Thus, in the Na⁺ solvation sphere it is possible to find the counterion from the salt in addition to the solvent molecules. The effect of various anions to stabilize the discharge products in different solvents has already been reported, where Lutz et al found that in weakly solvating solvents the increasing interaction of the anion ($ClO_4^- < PF_6$ $- < OTf^- < TFSi^-$) can stabilize the Na⁺ due to formation of contact ion pairs.[16] If both species (anion and solvent) present very different donor numbers (DNs), the species with the highest DN will occupy the cation coordination; consequently, it is possible that the anion can enter the first solvation sphere.

In this study, the effect of the salt counterion (ClO₄- anion) is disregarded due to its weak solvation effect on Na⁺.[15] Thus, it is possible to analyze the Na⁺ solvation as a function of glyme length and its effect on the electrochemical response in isolation. In any case, it is important to note that although the counterion does not affect either the solvation or the

formation mechanism of the discharge products on the cathode, it might have an important effect on the formation of the solid electrolyte interphase (SEI) on the surface of the metallic sodium anode.

Bearing in mind the importance of the chelating ability of glymes to Na⁺, it is crucial to understand the coordination structure of Na⁺ ion in the three studied solvents and its link to the electrochemical properties in Na-O₂ batteries. Computational modelling and its correlation with spectroscopy techniques are well suited to study this solvation phenomena.[32–34] DFT calculations were, therefore, first performed in order to shed light into the coordination structure.

Regarding the selection of the initial structures for the optimization procedures, it is known that glyme-based solvents prefer to curl when solvating alkaline ions.[27,35–37] In this way they are able to maximize the number of cation-O bonds, which compensates the energy penalty associated with dihedral rotations around C-O and C-C bonds. We therefore considered some plausible curled geometries as initial structures. Figure 1 shows the most stable optimized structures that we found with 1, 2, 3, or 4 solvents (depending on solvent) coordinated with the sodium ion. Upon adding glyme molecules to the solvation complex, more molecules can be included within the first solvation shell if linear glymes are considered. Of course, upon finite temperature, countless configurations can be explored, which are not explicitly calculated here. Instead, we aim at capturing the basic chemistry of glyme-Na⁺ interactions involved in the solvation of Na⁺ in glyme solvents which is key to understanding the mechanism through which the discharge and charge processes occur in Na-O₂ batteries.

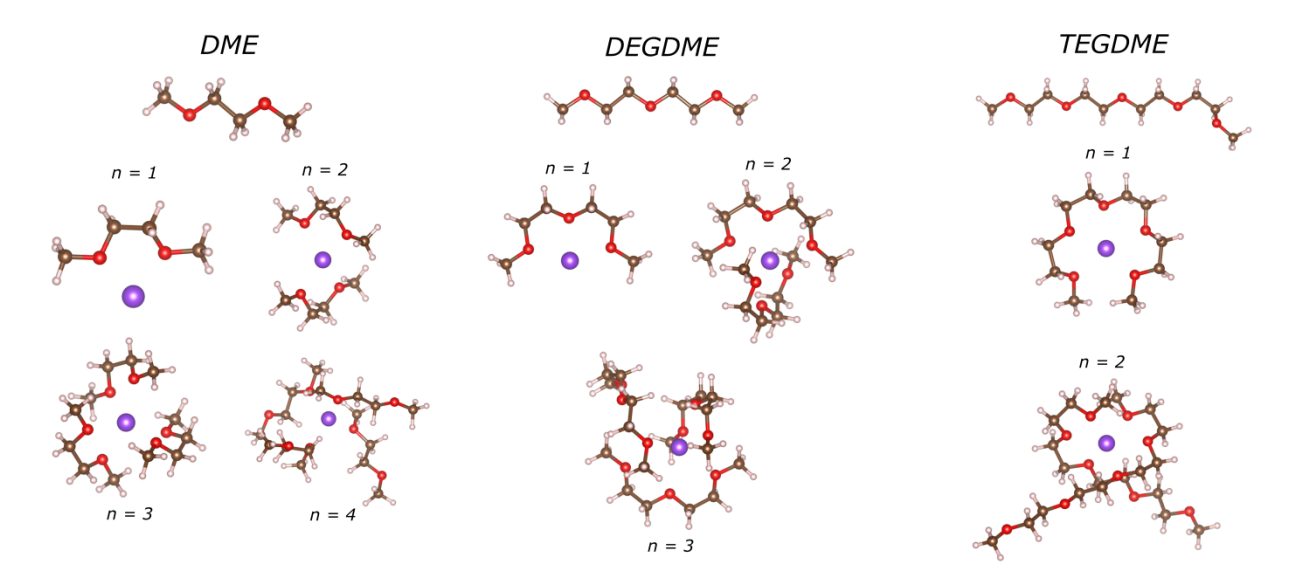


Figure 1: DFT optimized structures of isolated DME, DEGDME, and TEGDME solvent molecules and corresponding Na-solvent complexes containing n glyme molecules.

Using DFT, we predicted the shifts in the vibrational modes of C-O bonds within the glyme molecules as a function of the number of molecules (*n*) in the optimized complexation [Na-(DME)n]+, [Na-(DEGDME)n]+, and [Na-(TEGDME)n]+ clusters depicted in Figure 1. The greatest shifts are in the C-O-C stretching region (1200-1000 cm⁻¹) and the C-C-O twisting/bending region (900-800 cm⁻¹); Figure 2 shows the simulated infrared spectra specifically focusing on these two regions. Additionally, the calculated chemical shift in the C-C-O stretch between the isolated glyme molecule and a fully coordinated Na⁺ ranges from 35-50 cm⁻¹. We observed that on a per molecule basis, the relative intensities of the peaks are quite close, within 10%; this is important for the analysis of the experimental FTIR data, as it suggests that the adsorption coefficients can be approximated as being concentration independent.

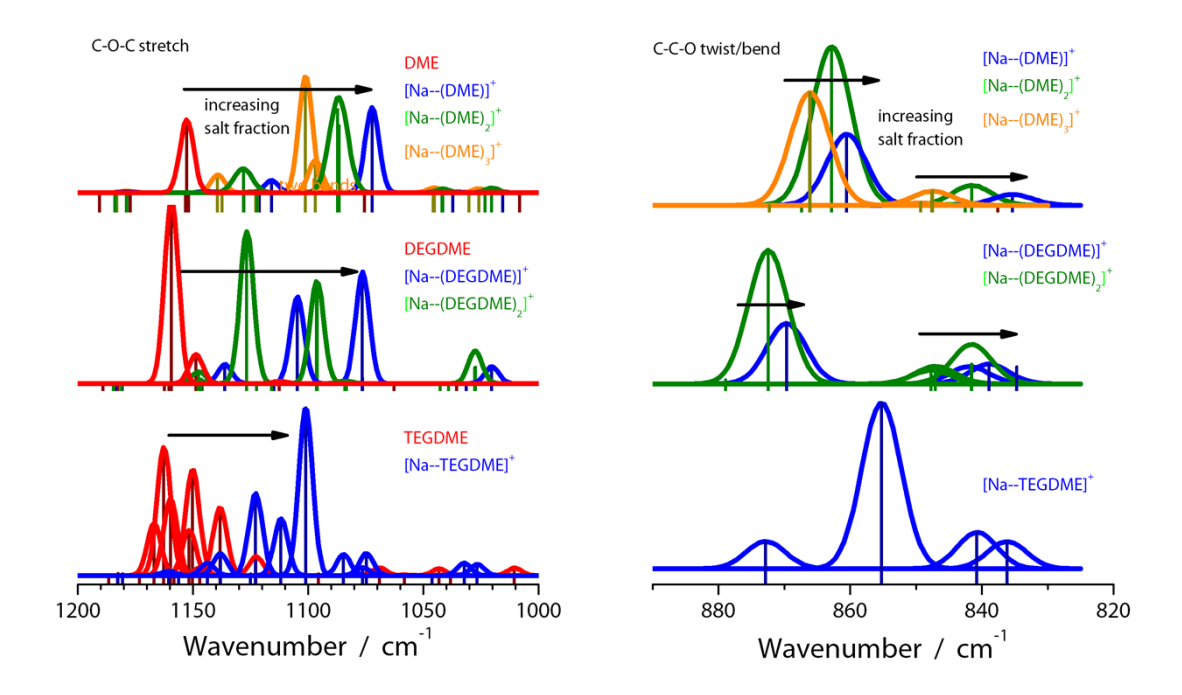


Figure 2. Simulated infrared spectra of the glyme molecules and complexes from the DFT results in Figure 1. Left-most plots focus on the C-O-C stretching region, while the right-most plots display the C-C-O bending/twisting modes. The arrows follow resonance wavenumber shift due to solvent-ion coordination with increasing Na ion mole fraction (relative concentration). From bulk DME to tightly bound glyme, the C-O-C stretch shows a red shift, while the C-C-O twist shows a blue.

Reaction energy landscapes for the formation of solvation complexes, based on n = 1, 2, 3 or 4 coordinating molecules, are shown in Figure 3. The energy profile in black is obtained by continuously adding solvent molecules to a given solvation complex in the calculation, whereas, the red energy profile shows the energy gain (or loss) when a single ion chelates with a single solvent molecule (M). The energies of the first step to obtain both black and red profiles are obtained as follows:

$$\Delta G_1^{r,b} = G([Na-M]^+) - G(M) - G(Na^+)$$
 Equation 1

The successive steps in the red energy profile are just a repetition of the first step $\Delta G_n^r = n \Delta G_1^{r,b}$, while for the black profile we consider:

$$\Delta G_n^b = G([Na - (M)_n]^+) - G([Na - (M)_{n-1}]^+) - G(M)$$
 Equation 2

where G is the Gibbs free energy of the the different configurations appearing in Figure 1. Here, we approximated it as $G = E_{DFT} + F_{vib}(T) + F_{rot}(T)$, where to the total DFT energy (E_{DFT}) the harmonic vibrational (F_{vib}) and rigid-body rotational (F_{rot}) computed free energies are added, considering T = 298 K.

A key observation is that when we continuously add glyme molecules to a $[Na-(M)_n]^+$ complex, the structure is further stabilized up to a threshold that decreases with the size of the solvent molecules: n = 3 for DME, n = 2-3 for DEGDME, and n = 1-2 for TEGDME. We note that previously proposed structures based on molecular dynamics (MD) simulations[27] are consistent with our findings, in particular the minima of the black energy profile in Figure 3. This is somewhat obvious, since smaller molecules allow for increasing the number of stabilizing Na-O bonds before solvent-solvent interactions begin to dominate, when compared to, for example TEGDME, where already a single molecule almost entirely chelates the Na ions, as can be seen in Figure 1. On the other hand, the red energy profile shows that it is thermodynamically preferred to chelate the Na ions to form isolated [Na—(M)]⁺ dimers where only a single solvent molecule is present. These results qualitatively explain the decrease in coordination number (i.e., number of molecules in the first coordination sphere) upon increasing the salt concentration in the mixture detailed below, assuming that at higher concentrations less solvent molecules are available to solvate each Na ion. We also note that at the more dilute limit, the experimental values for the solvation number do not coincide with the theoretical ones, which are underestimated. We argue that, although the black energy profile shows a minima at n = 3 for DME, n = 2-3 for DEGDME, and n = 1-2 for TEGDME, further increasing the amount of glyme molecules involved in the formation of the complex is still more favourable than not forming the complexes at all, so if we were to keep adding glyme molecules we could still get a thermodynamically favourable reaction. This, of course, would

require explicitly including a second solvation shell and thoroughly exploring the configurational space for such complexes, which is out of the scope in this study and will require an in-depth sampling of much larger complexes or applying MD-based simulations.

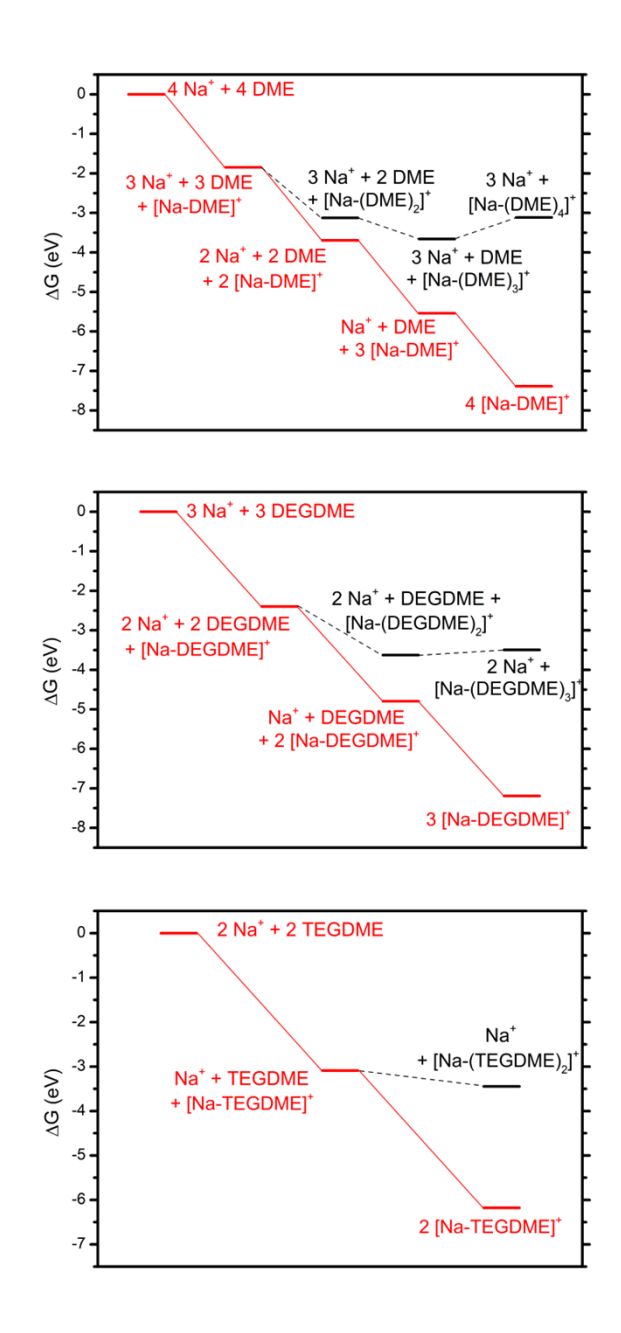


Figure 3. DFT reaction energies for the formation of $[Na-(M)_n]^+$ complexes (black curve), or the formation of $n[Na-(M)]^+$ isolated dimers (red curve). Values are in eV.

Experimentally, the coordination structure of the Na⁺ ions in the NaClO₄/DME-DEGDME-TEGDME solutions was estimated by processing the spectroscopy data through fitting the vibrational modes that are sensitive to the change in chemical environment due to ion association (*i.e.*, experience a significant electrostatic attraction to the Na⁺ ion),[38,39] as predicted with the DFT calculations. FTIR spectra with different NaClO₄ concentrations were recorded at ~21 °C and Table SI2 summarizes the concentration and molar ratios of the NaClO₄ salt and glyme-based solvents.

Assuming that the absorption coefficient is unaffected (sometimes an overreaching assumption to be sure) we can compare the area under the spectral signals due to uncoordinated or free solvent molecules (A_{free}) and those due to cation binding (A_{co}). The concentration of coordinating molecules (C_{co}) is a function of the concentration of the ions, in our case Na⁺ (C_{Na}).[40]

$$C_{co} = C_n \cdot C_{Na}$$
 Equation 3

Here, C_n is the apparent coordination number and is itself a function of C_{Na} and refers to the number of molecules of solvent per Na⁺ that either directly participates in coordination or whose chemical environment is affected by the charge (e.g., secondary solvation shells). C_n can be solved using the integrated intensities and the mole fraction of the mixture.[40]

$$C_n = \frac{A_{\text{co}} \quad C_{\text{total}}}{A_{\text{co}} + A_{\text{free}} C_{\text{Na}}}$$
 Equation 4

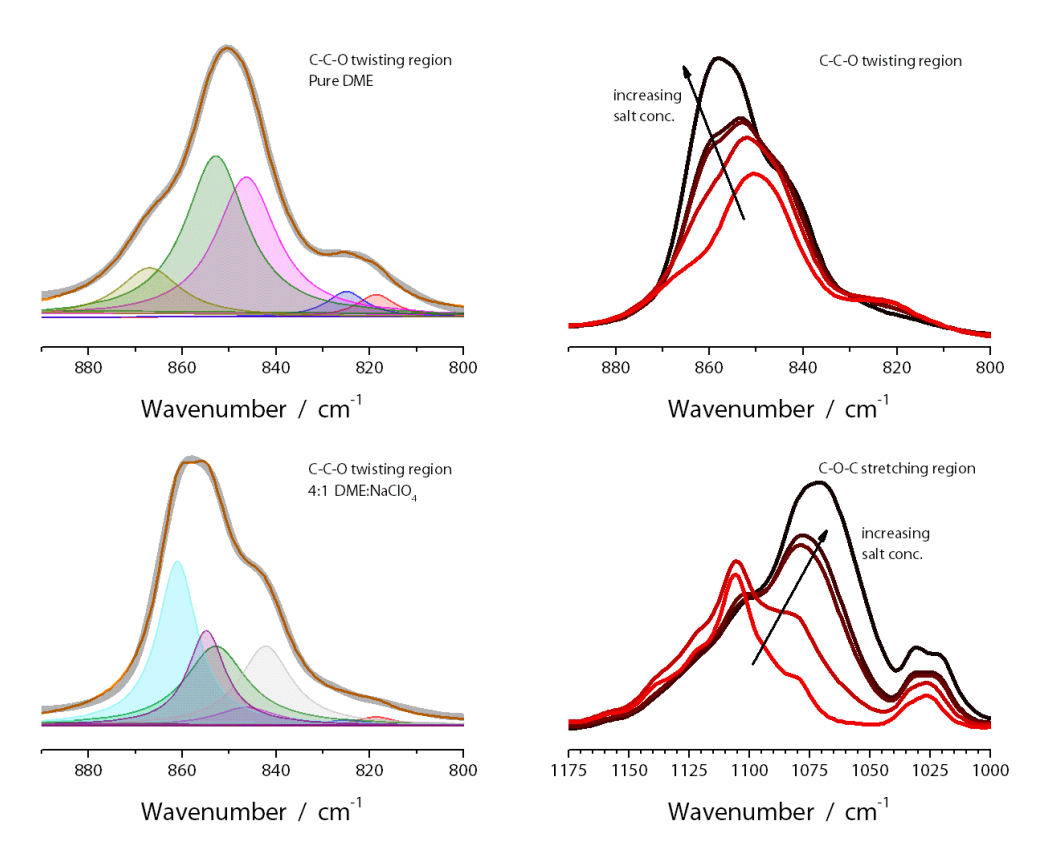


Figure 4. Left-most plots show Lorenzian deconvolution of the C-C-O bending/twisting region in the FTIR-ATR spectra: neat DME on top and 0.2 mole fraction in DME (moles of NaClO₄/ total mole of solution) on bottom. Right-most plots highlight the blue and red shift of the C-C-O bend/twist (top) and C-O-C stretch (bottom), respectively, due to coordination of Na⁺.

Figure 4 shows the representative fits of the FTIR spectra of the neat DME and most concentrated electrolyte about the C-O-C stretch at 1110 cm⁻¹ and the C-C-O bend/twist at 853 cm⁻¹. It is obvious that the deconvolution of the latter holds less uncertainties as there is less mixing of various vibrational modes. The 850 cm⁻¹ region of the neat DME can be fit to 5 peaks, while the 1100 cm⁻¹ region must be fitted to at least 8 peaks. Also, the perchlorate ion has a vibrational signal at 1095 cm⁻¹,[41] which is similar to the C-O-C stretches of the neat molecule. We can clearly see that there is a red shift in the C-O-C stretch which suggests electron donation of the oxygen to Na⁺, however further quantification is difficult due to the emergence of more signals. That said the red shift can be estimated as being approximately 30

cm⁻¹, 25 cm⁻¹ and 21 cm⁻¹ for DME, DEGDME, and TEGDME, respectively, which is similar to that predicted by DFT calculations in Figure 2. Turning to the C-C-O bend/twist, there is a clear blue shift upon coordination with Na⁺. The blue shift is the result of the changing dipole of the C-O bond, that is the mirror of the red shift seen in the C-O-C stretch. In other words, the interaction of the chelating oxygen on the Na⁺ weakens the bond with the adjacent carbons; and in response the C-C bonds are shortened producing the blue shift of the 853 cm⁻¹ peak to 861 cm⁻¹.

Apparent coordination numbers shown in Figure 5 were obtained using Equation 4 by analysing the relative ratio between the C-C-O bend stretch of uncoordinated and coordinated glyme, as discussed above. The apparent coordination numbers show an exponential decay to a near constant value at high salt loading. The coordination number are estimated to be 2 for DME and DEGDME and 1 for TEGDME. DMSO is shown as a baseline for the reproducibility of the technique, with an estimated coordination number of 3, and agrees with previous reports.[42] DMSO has a dipole moment of 4.0 D[43] while the glymes are 1.6, 1.9, and 2.4 D for DME, DEGDME and TEGDME, respectively.[44,45]

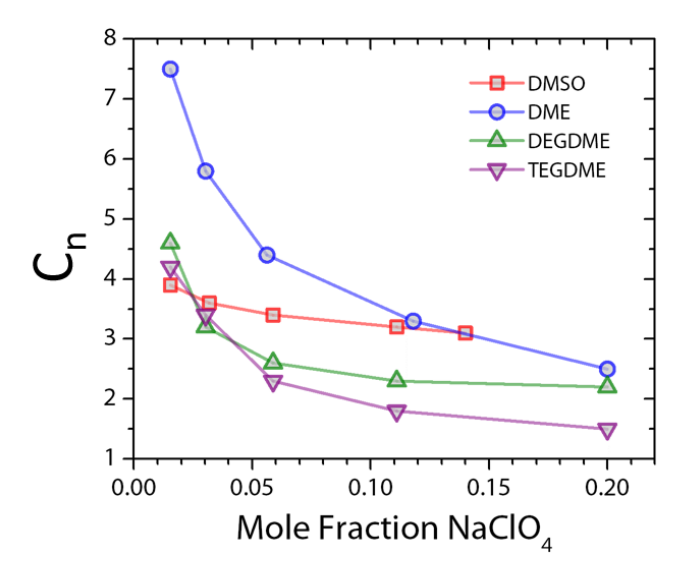


Figure 5. Apparent coordination number as a function of Na salt concentration (Mole fraction $NaClO_4 = moles of NaClO_4 / total moles)$

This means that effective charge screening of the cation is strongest for DMSO and weakest for DME. Thus, the glymes show a significantly elongated decay. It is worth noting that the effective coordination number of DEGDME reaches a constant value "faster" than the other glymes, with DME having not yet reached a "steady" value. DMSO also has greater Gutmann acceptor (AN, ~19 kcal mol⁻¹) and donor numbers (DNs, ~30 kcal mol⁻¹) than the glymes; thus, more stable solvation complexes are formed in DMSO with both anions and cations than in glymes[46]. The Gutmann donor number or "donicity" is a quantitative measure of the nucleophilic properties of a solvent, i.e., it provides information about the ability of a solvent to solvate other species. DN was defined as the negative ΔH -value for the formation of a 1:1 adduct between SbCl₅ and the molecules of a certain solvent in a dilute solution of 1,2dichloroethane.[47] The acceptor number, however, represents a quantitative and sensitive measurement of the electrophilic properties of a given solvent and it is calculated based on the ³¹P-NMR chemical shift of triethylphosphine oxide in the solvent.[47] In brief, the DN and AN values are a measure of the strength of solvents such as Lewis bases or acids, respectively. According to Meyer et al., the differences in acceptor and donor number values between the glymes are small, as shown in Table 1.[46] This is supported by the blue shift of the C-C-O bend/twist being the same for each glyme, ~ 8 cm⁻¹, as well as a similar red shift in the C-C-O stretch ~25 cm⁻¹. Therefore, simple charge screening and donor numbers-based arguments cannot explain differences in electrochemical kinetics of Na-O₂ systems. That is, entropic and kinetic terms may play a more dominant role by regulating configuration dynamics, viscosity, and bulk transport that in turn governs solvation/desolvation and ion exchange.

Table 1 – Gutmann's acceptor (AN) and donor numbers (DN) described in literature.

Solvent	AN [46,48]	DN (kcal/mol)[49]	DN (kcal/mol)[16]	DN (kcal/mol)[27]
DMSO	19.3	29.8	≈ 30	
DME	10.2	≈ 24	20.0	19 <u>+</u> 1
DEGDME	9.9		≈ 24	18 ± 1
TEGDME	10.5		16.6	12 ± 1

The obtained results in terms of coordination number are reasonable; as the C_n NaClO₄/ C_n solvent ratio increases, more Na⁺ and less solvent molecules for solvation will be present. It is, therefore, clear that establishing the right concentration of salt in each solvent is important in order to optimize the electrochemical response of the system. Depending on the number of molecules/coordinated bonds occurring in the solvation sphere, the stability of the Na⁺ - solvents pairs will change which in turn will influence the mechanism of formation of the discharge products which will be explored later.

Enthalpy of dissolution by calorimetry

The charge screening and donor numbers cannot clearly explain the differences in these three glymes; therefore, in order to understand the solubility and solvation characteristics of Na⁺ in glyme-based solvents, the enthalpies of dissolution ($\Delta H(\text{sol})$) were measured, for the first time in these systems, by calorimetry.

The energies for NaClO₄ in the three glyme-based solvents are shown in Table 2. The concentrations of NaClO₄ solutions used for this study are in the range of ≈ 0.02 -0.032 mol/L, which represents a molar fraction less than 0.015 (see Table SI2), and the FTIR data analysis indicates that the solutions are sufficiently dilute that the Na⁺ should be highly coordinated in all cases. The energies become more exothermic going from DME to DEGDME to TEGDME. The enthalpy and entropy of formation for NaClO₄ are reported as -382.75 kJ/mol and 142.26 J/molK, respectively.[50,51] The $\Delta H(\text{sol})$ values for these complexes are negative (exothermic reactions), suggesting that the formation of Na-glyme complexes is favourable, as the sum of the solvation enthalpies for Na⁺ and ClO₄⁻ is more negative than the lattice enthalpy of NaClO₄ for each solvent.

Table 2. Enthalpy of dissolution values ($\Delta H(\text{sol})$) for the three studied glymes in NaClO₄ measured by calorimetry.

Solvent	Enthalpy of	error	Enthalpy of	error
	dissolution	(kJ/mol)	dissolution	(J/g)

	(kJ/mol)		(J/g)	
DME	-23.33	1.5	-190.6	12
DEGDME	-40.02	0.031	-326.9	0.26
TEGDME	-45.12	0.6	-368.5	4.9

The trends are consistent with more energetically favourable solvation for increasing chain length in linear polyethers. The highest absolute $\Delta H(\text{sol})$ value for the interaction of Na⁺ with the glymes is seen for Na⁺(TEGDME) complex. This reflects the fact that the higher the absolute magnitude of the free energy, the greater is the affinity for the Na⁺ in that solvent.[52] While thermodynamic information helps to identify a specific electrolyte formulation under equilibrium conditions, the kinetics of the reactions are key to determine the optimal electrolyte for a given system, which will be further explain in the next section.

Prior to understanding the impact of these three solvents on the electrochemistry, a summarized graphical description about the difference of DME, DEGDME and TEGDME is presented in Figure 6.

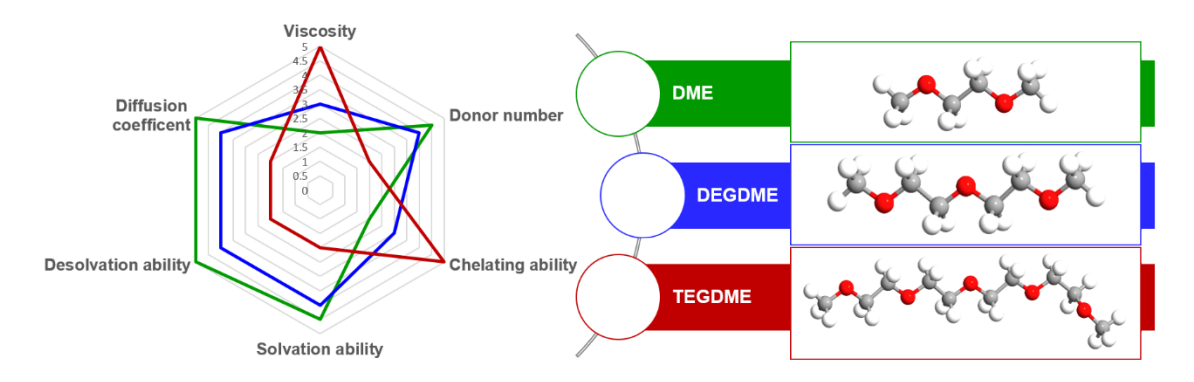


Figure 6. "Spider chart" to compare the physicochemical properties of the three studied solvents (DME, DEGDME and TEGDME).

Electrochemistry: ORR and cyclability tests

We first examine the ORR kinetics for the three studied glymes in Na-O₂ batteries (Figure SI1a). A single flat plateau is observed for the DME and DEGDME based electrolytes; whereas TEGDME shows an irregular profile. This finding is in agreement with that reported by Lutz et al. who observed a decrease in discharge capacity as increasing the glyme chain length.[27]

During the ORR process there are several factors to consider. First, the chelating ability of the glymes, which is greater as the chain length increases, as observed in the previously presented DFT and FTIR studies. This fact is rational, considering that the number of oxygen donor groups increases with the chain length: 2, 3 and 5 points for chelation for DME, DEGDME and TEGDME, respectively. Based on this, the higher the chelating effect of the solvent, the more "trapped" (stabilized) will be the Na⁺ in the electrolyte; in good agreement with the calorimetry data and DFT/FTIR results. Second, the superoxide species generated during ORR must stabilize in the solution, forming ion pairs, which is favored by the presence of longer chain solvents. However, the greater the ion pair stability, the more difficult the precipitation of the discharge products by electrolyte saturation. According to this hypothesis, the longer chain solvents should follow a solution-mediated mechanism; whilst decreasing the chelating ability of the solvent will result in a more surface-like process.[27] Likewise, a greater discharge capacity is expected for the solution-mediated process. However, this hypothesis is not fully met.[27] XRD data on the discharge electrodes (Figure SI1b) show NaO₂ formation in DME and DEGDME electrolytes; however, no signal is observed in TEGDME. In addition, SEM images confirmed (Figure SI2) the formation of cubic particles in the DME and DEGDME electrolytes, suggesting a solution-mediated mechanism; whereas a film-like structure is observed in TEGDME. These results are in good agreement with those reported in literature in Na-O₂ batteries.[27,53,54]

It is known that the solvation structure not only affects the dynamics and charge transfer of the electrolyte, but also the stability of some species. [55,56] In the case of TEGDME, the greater solvation of Na⁺ and stability of the $[Na^+(TEGDME)_n...O_2^-]$ complex leads to a greater energy to overcome the high desolvation barrier. At some point during discharge, TEGDME is not able to solvate more cations (*i.e.*, the release of chelated cations is kinetically limiting), which causes a precipitation of NaO₂ in film form or as cubes of very small size (Figure SI2). [27] In

this way, the surface is blocked with an insulating NaO₂ film causing premature cell death by electrode passivation. Therefore, in order to establish the formation mechanism of the discharge products, it is key to determine the right balance between the stability of the species $[Na^+(solvent)_n...O_2^-]$ and the capacity to desolvate.

Apart from the above-mentioned factors, the solubility of oxygen in the solvent (TEGDME < DEGDME < DME) and the viscosity (TEGDME > DEGDME > DME) (Table SI3) are other aspects that will affect the capacity of the discharge and the subsequent cyclability. The influence of the first factor is clear, the greater the solvent's ability to dissolve O_2 , the greater the capacity of the cell. In the case of the viscosity, there is an effect on the mobility of the species within the electrolyte, i.e., the higher the viscosity and the lower the oxygen solubility, the smaller the Nernst layer, which is directly related to the diffusion of the species in the region near to the surface of the electrode. In addition, the high viscosity hinders the supply of oxygen, especially at high current densities. For this reason, in the case of the TEGDME solvent, it has not been possible to conduct the study at higher current densities (120 μ A cm⁻²).

Regarding the charge process, one of the main factors to take into account is the re-solvation process. The discharge products from the electrode surface must be decomposed electrochemically during the OER and the species produced (Na⁺ and O₂-) must be re-stabilized in the electrolyte solution. Based on this, again the chelating ability of the solvent will determine this mechanism (TEGDME > DEGDME > DME). On the other hand, the diffusion of these species in the solvent will also be governed by the viscosity of the electrolyte, this diffusion being slower as the viscosity increases (TEGDME > DEGDME > DME).

In order to analyze the effect of the solvation/desolvation kinetics of the different glymes on the electrochemical response, cyclability studies have been conducted. In this study, the three glymes are analyzed at two different current densities (65 and 120 μ A cm⁻²) and two concentrations (0.1 and 1.5 M) of NaClO₄ salt. The results obtained are presented in Figure 7

(plots of voltage vs capacity during cycling are displayed in Figure SI3 in the supporting information).

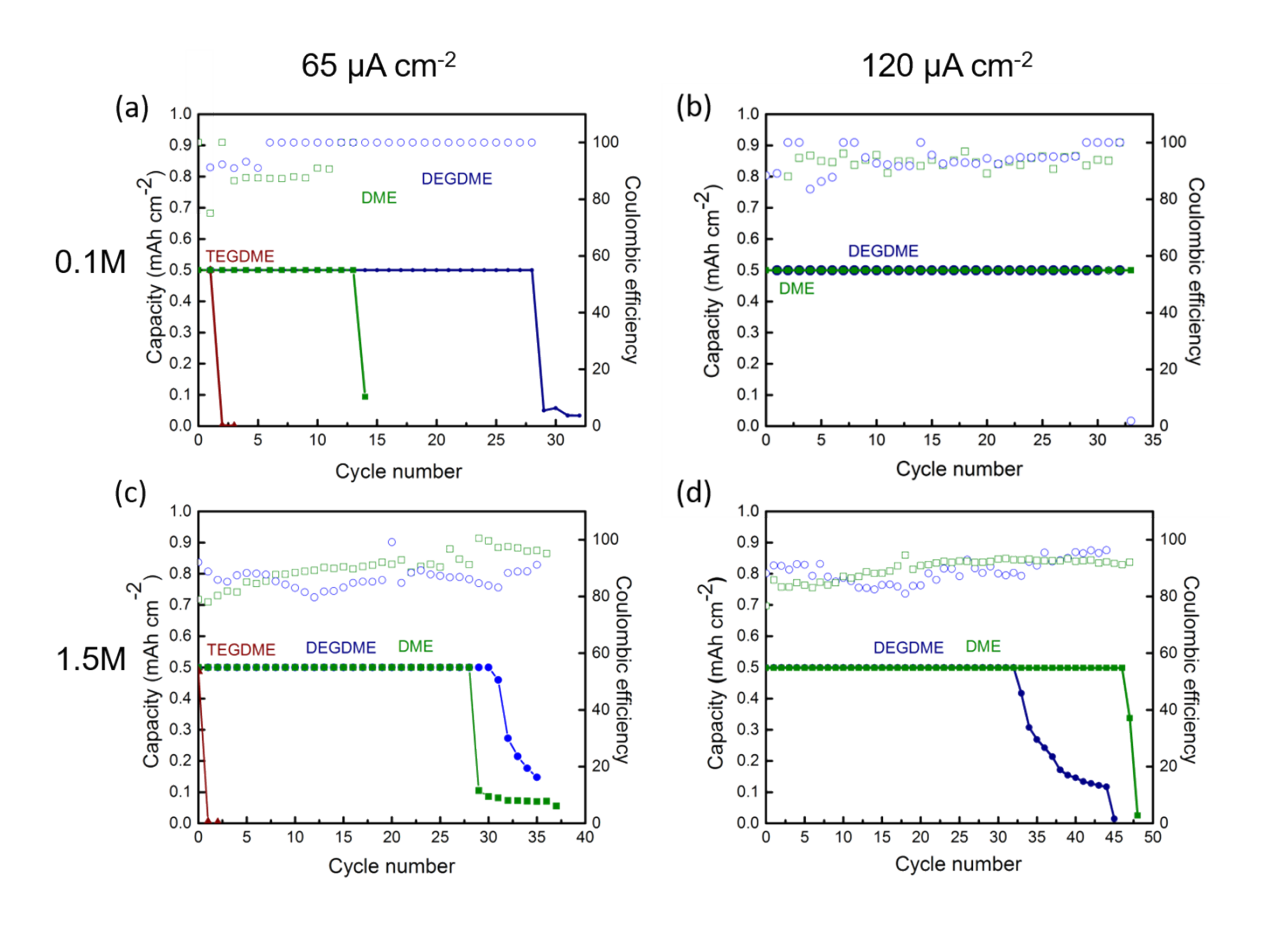


Figure 7. Cycling behaviour of Na-O₂ cells in different glymes containing to a fixed capacity $(0.5 \text{ mAh cm}^{-2})$ (a, b) 0.1 M and and (c, d) 1.5 M NaClO₄, at two current densities (65 and 125 μ A cm⁻²).

Analyzing the cyclability obtained for each system, at low salt concentrations (0.1 M NaClO₄) (Figure 7 a,b) the cyclability is higher with DEGDME, followed by DME and finally TEGDME, which cannot perform one complete cycle (Figure SI4a). This latter behaviour is due to two facts: (1) the high solvation barrier that must be overcome and (2) the high viscosity of the solvent (32.9 x 10⁻³ cm²/s at 25 °C)[57] which hinders the diffusion and mobility of the species. These factors affect the electrochemical response of the system to such extent that even when decreasing the current density, it is not possible to complete a single cycle. However, other parameters such as salt type, concentration and air cathode used might also play an

important role which has been observed by Li et al.[58] Regarding DME and DEGDME, their viscosities are much lower ($4.2 \times 10^{-3} \text{ cm}^2/\text{s}$ and $10.0 \times 10^{-3} \text{ cm}^2/\text{s}$ at 25 °C, respectively)[57]; therefore, it is possible to obtain higher cyclability even at higher intensities ($120 \times 65 \mu \text{A cm}^2$). Considering Figure 7a, the cell with DEGDME presents a more than acceptable cyclability completing 29 cycles, while in the case of the DME from the 13 cycle the cell begins to lose efficiency. In this way, the order of cyclability appears to be DEGDME > DME> TEGDME. To explain this trend, it is necessary to review the DN of these solvents, which vary according to the study (see Table 1).

Although there are certain discrepancies depending on the source, it is clear that the TEGDME presents the lowest DN; this solvent, therefore, will have more difficulty to dissolve the discharge products and the disproportionation will, subsequently, occur close to the electrode surface. In contrast, DME and DEGDME have comparable and higher DNs, which can be related to a greater facility to solubilize the NaO₂ generated during discharge. In the case of the DEGDME, this solvent presents the ideal balance between the ability to solvate/desolvate the Na⁺ and stabilize O₂⁻ by forming ion pairs (chelating ability), together with its ability to solubilize the discharge products (related to the DN), leading to a superior cyclability when compared with DME.

It is undeniable that the electrochemical behavior will be strongly linked to the solvation and desolvation processes in the electrolyte. As already mentioned, the DN is not the only factor that will govern these processes. The DN is a parameter that gives an idea of the Lewis basicity of a solvent, but there are other effects to consider as mentioned in the study conducted by Amine et al.[59] In this sense, it is important to consider both steric hindrance and the chelating effect of the solvent. In our study, the steric bulkiness of each solvent was taken into account when analyzing the most stable conformations in the different environments (see Figure 1). At lower salt concentration (i.e., 0.1M), there will be a greater number of electrolyte molecules to

solvate Na⁺, which will be shielded when surrounded by the solvent molecules. At the same number of solvent molecules, the arrangement of the molecules around the cation will be different due to the chain length (i.e., volume) of each solvent.

When comparing the situation of n = 3 in DME and DEGDME (see Figure 1), according to DFT calculations, in the case of DME the three molecules would use their donor oxygen atoms to solvate Na⁺. DEGDME, however, as a consequence of the steric hindrance and the greater volume of the solvent molecule itself, one of the molecules would use its three oxygen donor atoms, another molecule would use two, while the third only one. In both cases, the maximum coordination of Na⁺ (6) is fulfilled. Also, it should be noted that the more solvation positions a molecule utilizes, the greater the strength of the solvation. Bearing this in mind, although DEGDME is considered a better chelating agent than DME, in the situation of n = 3 only one of the molecules would act as a strong chelator of Na⁺, while the other two would chelate weaklier. This effect is captured in the black reaction energy curves (see Figure 3) of DME and DEGDME, as obtained with DFT, where, at n = 3, the DME complex is more stable relative to the DEGDME complex. As a consequence, the desolvation process is more favored for DEGDME than in the case of DME. This fact is also associated with the greater cyclability of the DEGDME cells at low current densities.

At higher current density (Figure 7b), DME cyclability increases from 14 to 30 cycles, and DEGDME from 29 to 32 cycles. By increasing the current intensity, the discharge process is faster and the electrolyte possess less time to stabilize the species through the formation of ion pairs $[Na^+(solvent)_n...O_2^-]$. In the case of DEGDME, this fact is aggravated due to its higher viscosity (more than double that of the DME), which prevents a sufficient diffusion of the species outside the Nernst layer. According to this result, at higher intensities, it is the viscosity of the solvent which governs the cycling behavior.

Recently, the use of electrolytes with high salt concentrations (> 3M) has become a hot topic, more intensively in Li-ion batteries.[60] High salt concentrations lead to a drastic change in the physico-chemical properties. Indeed, the interactions between cations, anions and the solvent are stronger. If the concentration is sufficiently high, between 3 and 5 M, a characteristic 3D solution structure is stabilized, which can provide greater interfacial stability.[61] Another key advantage of these electrolytes is the less corrosion of the electrodes at higher potentials due to the less amount of free solvent molecules.

In the case of Na-O₂ batteries, most of the solvent molecules will be coordinated when NaClO₄ in DEGDME is greater than 2 M, estimating that each Na⁺ will be solvated by two molecules of DEGDME.[62] This concentration (2 M) sets the limit between two situations. At lower concentrations, Na+ will be practically coordinated to solvent molecules. At higher concentrations, however, the counterion (ClO₄-) participates in the first coordination sphere, due to the smaller number of solvent molecules available. In order to avoid this second situation, a concentration of 1.5 M has been selected, without reaching a highly concentrated electrolyte. Regarding cyclability results, at low current density the use of DEGDME leads to a greater number of cycles (Figure 7c), 24 and 31 for DME and DEGDME, respectively. The highest cyclability achieved might be related to: (1) the increase in the ionic conductivity of the electrolyte and (2) the presence of less amount of free solvent molecules. The latter is associated with the appearance of side reactions, i.e., free solvent favors the gradual decomposition of the electrolyte. This behavior has already been observed by Park et al. when increasing the salt concentration.[62] They concluded that in more concentrated electrolytes, the NaO₂ discharge product is more stable and the appearance of side reactions is largely avoided.

At 0.1 M salt concentration, however, the DEGDME delivered more than twice as many cycles as DME; whereas at 1.5 M, the difference is not as pronounced. This fact can be related to the

number of molecules that surround the cation (Figure 5). At low salt concentrations, there is a greater availability of solvent molecules to solvate Na⁺, being $C_n = 7$ for the DME and 4 for the DEGDME. At higher salt concentrations, however, the availability of the molecules is more limited, approaching the $C_n = 2$ value in both systems, which will affect Na⁺ solvation process. In this new situation, the two molecules of DME will be coordinated to Na⁺ through the two donor oxygens, giving rise to a coordination of 4. In the case of DEGDME, the two molecules will be able to solvate the cation through its three donors, leading to a Na⁺ coordination of 6. While in more dilute electrolyte solutions, the desolvation of the DME is more complicated than for the DEGDME, at higher concentrations the DME presents a greater ability to desolvate, which is consistent with the DFT reaction free energies (see Figure 3). During charge, however, DEGDME facilitates, to a greater extent, the stabilization by dissolution in the electrolyte of the species produced in the decomposition of the discharge products. By increasing the current density (Figure 7d), the cyclability of DME is clearly higher than DEGDME (46 and 36 for DME and DEGDME, respectively). It has already been mentioned that at higher current densities, the viscosity of the solvent becomes a key parameter. In this case, as the salt concentration increases, there is also an increase in viscosity due to the formation of more Na⁺ ion-dipole interactions, which in fact may be stronger in DEGDME than DME (by higher dipole moment of the DEGDME - see table SI3).

CONCLUSIONS

The differing results regarding solvent selection in the literature hinders progress; without a detailed understanding of the role of Na⁺ solvation in the electrolyte it may be challenging to optimize the electrochemical performance. We have demonstrated that the size and dynamics of glymes affects charge/discharge rate in Na-O₂ batteries, and therefore the overall performance. From a dynamics point of view, the transport of Na⁺ is fastest in DME and slowest in TEGDME; this is essentially a viscosity effect. However, the desolvation energy

may be harder to overcome in DME as it shows less charge screening effect, that is, when a Na⁺ leaves or enters the system many DME molecules are to move about and that takes energy. DME is also seemingly less stable than the others. For TEGDME, it is slow, bulky, and has up to four chelation sites, which leads to sluggish Na⁺ transport and a high desolvation energy barrier. DEGDME seems to be the preferred solvent at both at low salt concentrations and high salt concentration/low rate because of its compromise in stability, viscosity, and coordination structure, which allows for best results in terms of transport and reaction kinetics. Following the path established in this work it should be possible to design new solvent/salt systems with properties suitable for other applications, i.e. low temperatures, Li-air, etc.

ACKNOWLEDGEMENTS

N.O.-V. and M.E would also like to thank the Basque Government for financial support through ELKARTEK project CICE20. This work was also financially supported by the "Ministerio de Economía y Competitividad" of Spain (under project MAT2016-78266-P), the "Fondo Europeo de Desarrollo Regional" (FEDER) and the Eusko Jaurlaritza/Gobierno Vasco (under project IT1226-19). Computer resources were provided by SGI/IZO-SGIker UPV/EHU (Arina cluster) and i2BASQUE academic network. FTIR measurements and their interpretation were supported by the U.S. Department of Energy, Office of Science, Basic Energy Sciences, Division of Materials Science and Engineering (RLS). A portion of this (FTIR, EC – RLS, GMV, Synthesis and Process Science Program; solvation energetics – CAB, Materials Chemistry Program) was supported by the U.S. Department of Energy, Office of Science, Basic Energy Sciences, Materials Sciences and Engineering Division.

BIBLIOGRAPHY

- [1] M.A. Hannan, M.M. Hoque, A. Mohamed, A. Ayob, Review of energy storage systems for electric vehicle applications: Issues and challenges, Renew. Sustain. Energy Rev. 69 (2017) 771–789. https://doi.org/10.1016/j.rser.2016.11.171.
- [2] D. Larcher, J.-M. Tarascon, Towards greener and more sustainable batteries for electrical energy storage., Nat. Chem. 7 (2015) 19–29. https://doi.org/10.1038/nchem.2085.
- [3] J.M. Tarascon, M. Armand, Issues and challenges facing rechargeable lithium batteries., Nature. 414 (2001) 359–67. https://doi.org/10.1038/35104644.
- [4] U.S. Department of the Interior, Mineral Commodity Summaries, USGS. (2016) 1–205.
- [5] X. Bi, R. Wang, K. Amine, J. Lu, A Critical Review on Superoxide-Based Sodium-Oxygen Batteries, Small Methods. 3 (2019) 1800247. https://doi.org/10.1002/smtd.201800247.
- [6] W.-W. Yin, Z.-W. Fu, The Potential of Na-Air Batteries, ChemCatChem. 9 (2017) 1545–1553.https://doi.org/10.1002/cctc.201600646.
- [7] B. Sun, C. Pompe, S. Dongmo, J. Zhang, K. Kretschmer, D. Schröder, J. Janek, G. Wang, Challenges for Developing Rechargeable Room-Temperature Sodium Oxygen Batteries, Adv. Mater. Technol. 3 (2018) 1800110. https://doi.org/10.1002/admt.201800110.
- [8] I. Landa-Medrano, I. Lozano, N. Ortiz-Vitoriano, I. Ruiz de Larramendi, T. Rojo, Redox mediators: a shuttle to efficacy in metal—O₂ batteries, J. Mater. Chem. A. 7 (2019) 8746–8764. https://doi.org/10.1039/C8TA12487F.
- [9] C.L. Bender, B. Jache, P. Adelhelm, J. Janek, Sodiated carbon: a reversible anode for sodium–oxygen batteries and route for the chemical synthesis of sodium superoxide (NaO₂), J. Mater. Chem. A. 3 (2015) 20633–20641. https://doi.org/10.1039/C5TA06640A.
- [10] P. Hartmann, M. Heinemann, C.L. Bender, K. Graf, R.-P. Baumann, P. Adelhelm, C. Heiliger, J. Janek, Discharge and Charge Reaction Paths in Sodium-Oxygen Batteries: Does NaO₂ Form by Direct Electrochemical Growth or by Precipitation from Solution?, J. Phys. Chem. C. 119 (2015) 22778–22786. https://doi.org/10.1021/acs.jpcc.5b06007.
- [11] I. Landa-Medrano, J.T. Frith, I. Ruiz de Larramendi, I. Lozano, N. Ortiz-Vitoriano, N. Garcia-Araez, T. Rojo, Understanding the charge/discharge mechanisms and passivation reactions in

- Na-O₂ batteries, J. Power Sources. 345 (2017) 237–246. https://doi.org/10.1016/j.jpowsour.2017.02.015.
- [12] I. Landa-Medrano, A. Sorrentino, L. Stievano, I. Ruiz de Larramendi, E. Pereiro, L. Lezama, T. Rojo, D. Tonti, Architecture of Na-O₂ battery deposits revealed by transmission X-ray microscopy, Nano Energy. 37 (2017) 224–231. https://doi.org/10.1016/j.nanoen.2017.05.021.
- [13] P. Hartmann, C.L. Bender, M. Vračar, A.K. Dürr, A. Garsuch, J. Janek, P. Adelhelm, A rechargeable room-temperature sodium superoxide (NaO₂) battery., Nat. Mater. 12 (2013) 228–32. https://doi.org/10.1038/nmat3486.
- [14] H. Yadegari, Y. Li, M. Norouzi Banis, X. Li, B. Wang, Q. Sun, R. Li, T.-K. Sham, X. Cui, X. Sun, On Rechargeability and Reaction Kinetics of Sodium-Air Batteries, Energy Environ. Sci. 7 (2014) 3747–3757. https://doi.org/10.1039/C4EE01654H.
- [15] L. Lutz, D. Alves Dalla Corte, M. Tang, E. Salager, M. Deschamps, A. Grimaud, L. Johnson, P.G. Bruce, J.M. Tarascon, Role of Electrolyte Anions in the Na–O₂ Battery: Implications for NaO₂ Solvation and the Stability of the Sodium Solid Electrolyte Interphase in Glyme Ethers, Chem. Mater. 29 (2017) 6066–6075. https://doi.org/10.1021/acs.chemmater.7b01953.
- [16] V.S. Dilimon, C. Hwang, Y.-G. Cho, J. Yang, H.-D. Lim, K. Kang, S.J. Kang, H.-K. Song, Superoxide stability for reversible Na-O₂ electrochemistry, Sci. Rep. 7 (2017) 17635. https://doi.org/10.1038/s41598-017-17745-9.
- [17] M. He, K.C. Lau, X. Ren, N. Xiao, W.D. McCulloch, L.A. Curtiss, Y. Wu, Concentrated Electrolyte for the Sodium–Oxygen Battery: Solvation Structure and Improved Cycle Life, Angew. Chemie - Int. Ed. 55 (2016) 15310–15314. https://doi.org/10.1002/anie.201608607.
- [18] C. Pozo-Gonzalo, P.C. Howlett, D.R. MacFarlane, M. Forsyth, Highly reversible oxygen to superoxide redox reaction in a sodium-containing ionic liquid, Electrochem. Commun. 74 (2017) 14–18. https://doi.org/10.1016/j.elecom.2016.11.010.
- [19] E. Azaceta, L. Lutz, A. Grimaud, J.M. Vicent-Luna, S. Hamad, L. Yate, G. Cabañero, H.J. Grande, J.A. Anta, J.M. Tarascon, R. Tena-Zaera, Electrochemical Reduction of Oxygen in Aprotic Ionic Liquids Containing Metal Cations: A Case Study on the Na–O₂ system, ChemSusChem. 10 (2017) 1616–1623. https://doi.org/10.1002/cssc.201601464.

- [20] Y. Zhang, N. Ortiz-Vitoriano, B. Acebedo, L. O'Dell, D.R. MacFarlane, T. Rojo, M. Forsyth, P.C. Howlett, C. Pozo-Gonzalo, Elucidating the Impact of Sodium Salt Concentration on the Cathode-Electrolyte Interface of Na-Air Batteries, J. Phys. Chem. C. 122 (2018) 15276– 15286. https://doi.org/10.1021/acs.jpcc.8b02004.
- [21] C. Pozo-Gonzalo, Y. Zhang, N. Ortiz-Vitoriano, J. Fang, M. Enterría, M. Echeverría, J.M. López del Amo, T. Rojo, D.R. MacFarlane, M. Forsyth, P.C. Howlett, Controlling the Three-Phase Boundary in Na–Oxygen Batteries: The Synergy of Carbon Nanofibers and Ionic Liquid, ChemSusChem. 12 (2019) 4054–4063. https://doi.org/10.1002/cssc.201901351.
- [22] B. Wang, N. Zhao, Y. Wang, W. Zhang, W. Lu, X. Guo, J. Liu, Electrolyte-controlled discharge product distribution of Na-O₂ battery: A combined computational and experimental study, Phys. Chem. Chem. Phys. 19 (2017) 2940–2949. https://doi.org/10.1039/C6CP07537A.
- [23] R. Black, A. Shyamsunder, P. Adeli, D. Kundu, G.K. Murphy, L.F. Nazar, The Nature and Impact of Side Reactions in Glyme-based Sodium-Oxygen Batteries, ChemSusChem. 9 (2016) 1795–1803. https://doi.org/10.1002/cssc.201600034.
- [24] H. Yadegari, M. Norouzi Banis, X. Lin, A. Koo, R. Li, X. Sun, Revealing the Chemical Mechanism of NaO₂ Decomposition by In Situ Raman Imaging, Chem. Mater. 30 (2018) 5156–5160 acs.chemmater.8b01704. https://doi.org/10.1021/acs.chemmater.8b01704.
- [25] L. Schafzahl, N. Mahne, B. Schafzahl, M. Wilkening, C. Slugovc, S.M. Borisov, S.A. Freunberger, Singlet Oxygen during Cycling of the Aprotic Sodium-O₂ Battery, Angew. Chemie Int. Ed. 56 (2017) 15728–15732. https://doi.org/10.1002/anie.201709351.
- [26] D. Sharon, D. Hirshberg, M. Afri, A.A. Frimer, D. Aurbach, The importance of solvent selection in Li–O₂ cells, Chem. Commun. 53 (2017) 3269–3272. https://doi.org/10.1039/C6CC09086A.
- [27] L. Lutz, W. Yin, A. Grimaud, D. Alves Dalla Corte, M. Tang, L. Johnson, E. Azaceta, V. Sarou-Kanian, A.J. Naylor, S. Hamad, J.A. Anta, E. Salager, R. Tena-Zaera, P.G. Bruce, J.M. Tarascon, High capacity Na-O₂ batteries: Key parameters for solution-mediated discharge, J. Phys. Chem. C. 120 (2016) 20068–20076. https://doi.org/10.1021/acs.jpcc.6b07659.
- [28] A.D. Becke, Density-functional thermochemistry. III. The role of exact exchange, J. Chem.

- Phys. 98 (1993) 5648–5652. https://doi.org/10.1063/1.464913.
- [29] C. Lee, W. Yang, R.G. Parr, Development of the Colle-Salvetti correlation-energy formula into a functional of the electron density, Phys. Rev. B. 37 (1988) 785–789. https://doi.org/10.1103/PhysRevB.37.785.
- [30] V. Blum, R. Gehrke, F. Hanke, P. Havu, V. Havu, X. Ren, K. Reuter, M. Scheffler, Ab initio molecular simulations with numeric atom-centered orbitals, Comput. Phys. Commun. 180 (2009) 2175–2196. https://doi.org/10.1016/j.cpc.2009.06.022.
- [31] V. Havu, V. Blum, P. Havu, M. Scheffler, Efficient O (N) integration for all-electron electronic structure calculation using numeric basis functions, J. Comput. Phys. 228 (2009) 8367–8379. https://doi.org/10.1016/j.jcp.2009.08.008.
- [32] J. Wahlers, K.D. Fulfer, D.P. Harding, D.G. Kuroda, R. Kumar, R. Jorn, Solvation Structure and Concentration in Glyme-Based Sodium Electrolytes: A Combined Spectroscopic and Computational Study, J. Phys. Chem. C. 120 (2016) 17949–17959. https://doi.org/10.1021/acs.jpcc.6b06160.
- [33] D. Monti, E. Jónsson, M.R. Palacín, P. Johansson, Ionic liquid based electrolytes for sodiumion batteries: Na+ solvation and ionic conductivity, J. Power Sources. 245 (2014) 630–636. https://doi.org/10.1016/j.jpowsour.2013.06.153.
- [34] A. V. Cresce, S.M. Russell, O. Borodin, J.A. Allen, M.A. Schroeder, M. Dai, J. Peng, M.P. Gobet, S.G. Greenbaum, R.E. Rogers, K. Xu, Solvation behavior of carbonate-based electrolytes in sodium ion batteries, Phys. Chem. Chem. Phys. 19 (2017) 574–586. https://doi.org/10.1039/C6CP07215A.
- [35] M. Callsen, K. Sodeyama, Z. Futera, Y. Tateyama, I. Hamada, The Solvation Structure of Lithium Ions in an Ether Based Electrolyte Solution from First-Principles Molecular Dynamics, J. Phys. Chem. B. 121 (2017) 180–188. https://doi.org/10.1021/acs.jpcb.6b09203.
- [36] Y. Sun, I. Hamada, Insight into the Solvation Structure of Tetraglyme-Based Electrolytes via First-Principles Molecular Dynamics Simulation, J. Phys. Chem. B. 122 (2018) 10014–10022. https://doi.org/10.1021/acs.jpcb.8b07098.
- [37] Y. Okamoto, Y. Kubo, Ab Initio Calculations for Decomposition Mechanism of CH₃O(CH₂

- $CH_2O)_N CH_3$ (N = 1-4) by the Attack of O_2 Anion, J. Phys. Chem. C. 117 (2013) 15940–15946. https://doi.org/10.1021/jp404849u.
- [38] C.M. Burba, R. Frech, Spectroscopic Measurements of Ionic Association in Solutions of LiPF₆, J. Phys. Chem. B. 109 (2005) 15161–15164. https://doi.org/10.1021/jp058045f.
- [39] D.M. Seo, S. Reininger, M. Kutcher, K. Redmond, W.B. Euler, B.L. Lucht, Role of Mixed Solvation and Ion Pairing in the Solution Structure of Lithium Ion Battery Electrolytes, J. Phys. Chem. C. 119 (2015) 14038–14046. https://doi.org/10.1021/acs.jpcc.5b03694.
- [40] D.M. Seo, O. Borodin, S.-D. Han, P.D. Boyle, W.A. Henderson, Electrolyte Solvation and Ionic Association II. Acetonitrile-Lithium Salt Mixtures: Highly Dissociated Salts, J. Electrochem. Soc. 159 (2012) A1489–A1500. https://doi.org/10.1149/2.035209jes.
- [41] F.A. Miller, C.H. Wilkins, Infrared Spectra and Characteristic Frequencies of Inorganic Ions, Anal. Chem. 24 (1952) 1253–1294. https://doi.org/10.1021/ac60068a007.
- [42] M. He, K.C. Lau, X. Ren, N. Xiao, W.D. McCulloch, L.A. Curtiss, Y. Wu, Concentrated Electrolyte for the Sodium–Oxygen Battery: Solvation Structure and Improved Cycle Life, Angew. Chemie - Int. Ed. 55 (2016) 15310–15314. https://doi.org/10.1002/anie.201608607.
- [43] A.E. Pekary, Dipole moment and far-infrared studies on the dimethyl sulfoxide-iodine complex, J. Phys. Chem. 78 (1974) 1744–1746. https://doi.org/10.1021/j100610a013.
- [44] S. Tang, H. Zhao, Glymes as versatile solvents for chemical reactions and processes: from the laboratory to industry, RSC Adv. 4 (2014) 11251–11287. https://doi.org/10.1039/c3ra47191h.
- [45] K. Kimura, R. Fujishiro, The Dipole Moments of the Oligether of Ethylene Glycol, Bull. Chem. Soc. Jpn. 39 (1966) 608–610. https://doi.org/10.1246/bcsj.39.608.
- [46] U. Mayer, V. Gutmann, W. Gerger, The acceptor number? A quantitative empirical parameter for the electrophilic properties of solvents, Monatshefte Für Chemie. 106 (1975) 1235–1257. https://doi.org/10.1007/BF00913599.
- [47] V. Gutmann, E. Wychera, Coordination reactions in non aqueous solutions The role of the donor strength, Inorg. Nucl. Chem. Lett. 2 (1966) 257–260. https://doi.org/10.1016/0020-1650(66)80056-9.
- [48] C.O. Laoire, S. Mukerjee, K.M. Abraham, E.J. Plichta, M. a. Hendrickson, Influence of

- Nonaqueous Solvents on the Electrochemistry of Oxygen in the Rechargeable Lithium–Air Battery, J. Phys. Chem. C. 114 (2010) 9178–9186. https://doi.org/10.1021/jp102019y.
- [49] V. Gutmann, Solvent effects on the reactivities of organometallic compounds, Coord. Chem. Rev. 18 (1976) 225–255. https://doi.org/10.1016/S0010-8545(00)82045-7.
- [50] J. M. W. Chase, NIST-JANAF Themochemical Tables, 4th edition, J. Phys. Chem. Ref. Data, Monograph 9., 1998.
- [51] NIST Chemistry WebBook, NIST Standard Reference Database Number 69 March 2003 Release, www version: http://webbook.nist.gov/chemistry., n.d.
- [52] G. Kamath, R.W. Cutler, S.A. Deshmukh, M. Shakourian-Fard, R. Parrish, J. Huether, D.P. Butt, H. Xiong, S.K.R.S. Sankaranarayanan, In silico based rank-order determination and experiments on nonaqueous electrolytes for sodium ion battery applications, J. Phys. Chem. C. 118 (2014) 13406–13416. https://doi.org/10.1021/jp502319p.
- [53] M. Enterría, C. Botas, J.L. Gómez Urbano, B. Acebedo, J.M. López del Amo, D. Carriazo, T. Rojo, N. Ortiz-Vitoriano, Pathways Towards High Performance Na-O2 Batteries: Tailoring Graphene Aerogel Cathode Porosity & Nanostructure, J. Mater. Chem. A. 6 (2018) 20778–20787. https://doi.org/10.1039/C8TA07273F.
- [54] N. Ortiz-Vitoriano, T.P. Batcho, D.G. Kwabi, B. Han, N. Pour, K.P.C. Yao, C. V. Thompson, Y. Shao-Horn, Rate-Dependent Nucleation and Growth of NaO 2 in Na-O 2 Batteries, J. Phys. Chem. Lett. 6(13) (2015) 2636–2643. https://doi.org/10.1021/acs.jpclett.5b00919.
- [55] S. Perkin, B. Kirchner, M.D. Fayer, Preface: Special Topic on Chemical Physics of Ionic Liquids, J. Chem. Phys. 148 (2018) 193501. https://doi.org/10.1063/1.5039492.
- [56] N.N. Rajput, X. Qu, N. Sa, A.K. Burrell, K.A. Persson, The Coupling between Stability and Ion Pair Formation in Magnesium Electrolytes from First-Principles Quantum Mechanics and Classical Molecular Dynamics, J. Am. Chem. Soc. 137 (2015) 3411–3420. https://doi.org/10.1021/jacs.5b01004.
- [57] A. Pal, Y.P. Singh, Viscosity in Water + Ethylene Glycol Dimethyl, +Diethylene Glycol Dimethyl, +Triethylene Glycol Dimethyl, and +Tetraethylene Glycol Dimethyl Ethers at 298.15 K, 41 (1996) 1008–1011. https://doi.org/10.1021/JE950299E.

- [58] N. Li, Y. Yin, F. Meng, Q. Zhang, J. Yan, Q. Jiang, Enabling Pyrochlore-Type Oxides as Highly Efficient Electrocatalysts for High-Capacity and Stable Na–O₂ Batteries: The Synergy of Electronic Structure and Morphology, ACS Catal. 7 (2017) 7688–7694. https://doi.org/10.1021/acscatal.7b02074.
- [59] C.C. Su, M. He, R. Amine, T. Rojas, L. Cheng, A.T. Ngo, K. Amine, Solvating power series of electrolyte solvents for lithium batteries, Energy Environ. Sci. 12 (2019) 1249–1254. https://doi.org/10.1039/c9ee00141g.
- [60] Y. Yamada, J. Wang, S. Ko, E. Watanabe, A. Yamada, Advances and issues in developing salt-concentrated battery electrolytes, Nat. Energy. 4 (2019) 269–280. https://doi.org/10.1038/s41560-019-0336-z.
- [61] J. Zheng, J.A. Lochala, A. Kwok, Z.D. Deng, J. Xiao, Research Progress towards Understanding the Unique Interfaces between Concentrated Electrolytes and Electrodes for Energy Storage Applications, Adv. Sci. 4 (2017) 1700032. https://doi.org/10.1002/advs.201700032.
- [62] H. Park, J. Kim, M.H. Lee, S.K. Park, D.-H. Kim, Y. Bae, Y. Ko, B. Lee, K. Kang, Highly Durable and Stable Sodium Superoxide in Concentrated Electrolytes for Sodium-Oxygen Batteries, Adv. Energy Mater. 8 (2018) 1801760. https://doi.org/10.1002/aenm.201801760.